New look at magnetism in single-crystal Gd-Y alloys

T. Ito,* S. Legvold, and B. J. Beaudry
Ames Laboratory-U.S. DOE and Department of Physics, Iowa State University, Ames, Iowa 50011
(Received 29 September 1980)

Magnetic susceptibility, electrical resistivity, and specific-heat measurements have been made on a number of polycrystalline and single-crystal samples of Gd-rich Gd-Y alloys. It has been found (1) that samples with more than 30 at.% Y exhibit a helical structure phase, (2) that samples between 10 and 30 at.% Y exhibit two different Curie-Weiss regimes leading to "double" ferromagnetism, and (3) that samples with less than 10 at.% Y have Gd-like behavior.

I. INTRODUCTION

In one of the first intra-rare-earth alloy systems investigated magnetically Thoburn *et al.*[1] found that samples with more than 40 at.% Y in Gd exhibited antiferromagnetism while samples with less than 33 at.% Y were ferromagnetic. A number of subsequent studies[2–6] have more or less corroborated these early findings. More recently, in a search for Lifshitz points in rare-earth alloys at low applied fields, Legvold *et al.*[7] found peculiar isofield behavior for polycrystalline samples having 28 and 30 at.% Y. These observations prompted the present detailed study of the Gd-Y system with emphasis on single crystals for clarity in the observations. Some of the results reported here have been published in a Letter.[8]

II. SAMPLE PREPARATION

High-purity Gd and Y in proper proportion were arc melted together into small buttons over a water-cooled copper hearth in a purified argon atmosphere. The buttons were inverted and re-arc melted several times to ensure homogeneity. The polycrystalline samples used were $3 \times 3 \times 5$ mm^3 rectangular parallelepipeds cut from the arc-melted buttons.

The single-crystal specimens were grown by the annealing process described by Nigh.[9] In most instances the annealing time was 3 days at a temperature of 1600 K. Back reflection Laue x-ray patterns were used to find the principal axes of the hcp crystals. Insofar as possible the sample dimensions were $3 \times 3 \times 5$ mm^3, with the long dimension oriented along the crystallographic axis to be placed in the direction of the magnetic field for the magnetization studies. It was found by experiment that such rectangular samples would yield results identical (within experimental error) to those for single-crystal spheres.

Chemical analysis of selected samples showed that the constituent Gd and Y masses going into a button were reliable in determining the alloy composition to about 0.1 at.%. Hence the weighed-in masses were used for determining sample composition.

III. MAGNETIZATION RESULTS

The magnetization results will be presented first because they give the most significant information. In Fig. 1 we give the isofield results at about 30 Oe applied field for polycrystalline samples of pure Gd and of Gd alloyed with 5, 10, 15, 20, and 25 at.% Y. Also shown are *a*-axis single-crystal data for samples containing 30 and 34 at.% Y. The magnetic moment (ordinate) scale for each sample has been shifted as indicated in order to give an orderly display. There was no observable basal-plane anisotropy in any of the samples explored for this phenomenon; however, considerable twofold anisotropy between *a*- and *c*-axis samples was found as will be seen subsequently. We have used the *a*-axis results for the 30 and 34 at.% Y samples in Fig. 1 because the weighting factor would

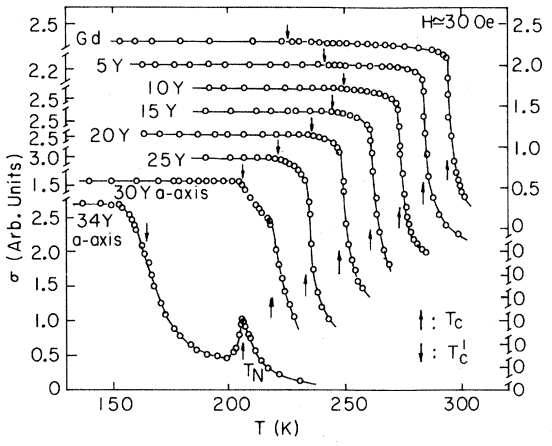

FIG. 1. Magnetization vs temperature for most of the alloys studied. Single crystal *a*-axis data are shown for the 30 and 34 at.% Y samples while the other data are for polycrystalline samples.

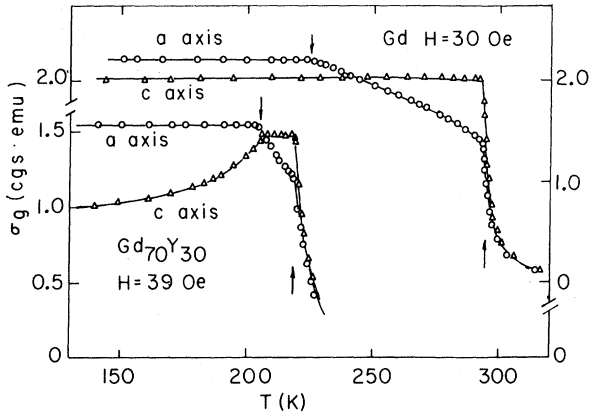

FIG. 2. Magnetization vs temperature for the pure Gd and 30 at.% Y in Gd single-crystal samples.

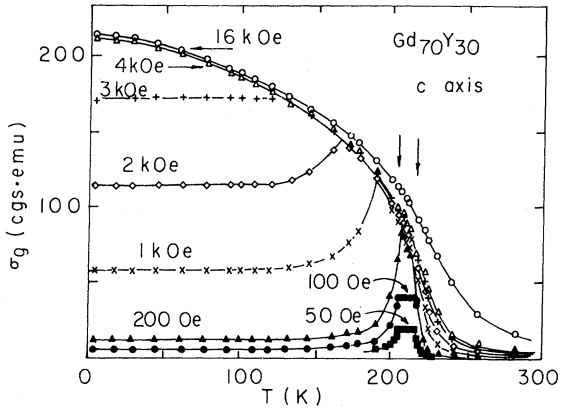

FIG. 4. Isofield magnetization vs temperature data for 30 at.% Y along the *c* axis.

be two for an *a* axis as compared to one for the *c* axis in estimating polycrystalline results from single-crystal data.

Several features of the data of Fig. 1 are significant. (1) For all samples the isofield magnetization is constant as the temperature decreases below the lowest ordering temperature. This indicates uniform domain structure and free pole energy prevails for the system. (2) As *Y* is added the highest ordering temperature, indicated by upward pointing arrows, decreases monotonically as might be expected and beyond about 32 at.% Y helical ordering occurs. (3) There is a second (lower) ordering temperature T_C^1 which is indicated by downward pointing arrows. For pure Gd this is the temperature at which the easy direction has moved to a direction close to the basal plane from the *c*-axis direction. From the appearance of the data around the knee this same behavior is presumed to obtain for the 5 at.% Y sample. The change in the shape of the knee for 10 at.% Y suggests that a new type of magnetic ordering has been encountered which extends out to 30 at.% Y and which has been examined in detail at the latter concentration. The steadily decreasing T_C^1 temperature with increasing *Y* concentration about 10 at.% should be noted in this connection. (4) At 34 at.% Y (and above) the onset of antiferromagnetism is indicated by the Néel point cusp.

The isofield magnetization data for pure Gd and for 30 at.% Y in Gd, as previously presented,[8] are shown in Fig. 2. It can be seen that for pure Gd the magnetic moment shows Curie-Weiss growth with decreasing temperature for both *a*-axis and *c*-axis samples down to the T_C of 293.6 K. Below T_C the *a*-axis moment increases with decreasing temperature with a slight concave downward behavior because of twofold magnetic anisotropy which forces the easy direction of magnetization to change from along the *c* axis to along the *a* axis. For the 30 at.% Y sample the data are like those for Gd down to a T_C of 218.8 K

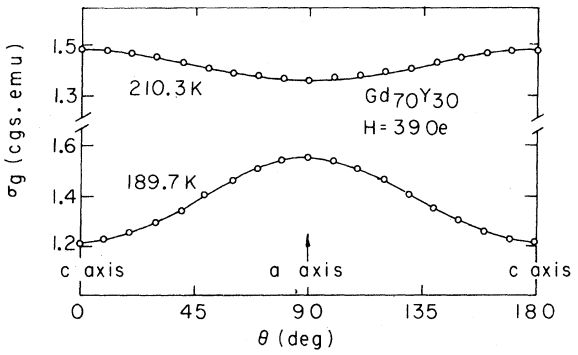

FIG. 3. Magnetization vs angle in the *c*-*a* plane for the 30 at.% Y sample. The data show twofold anisotropy which is different at the two different temperatures.

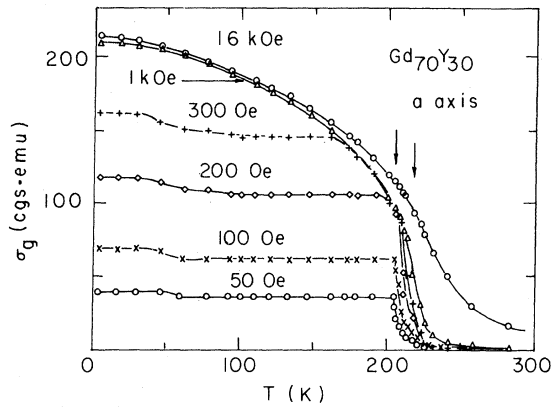

FIG. 5. Isofield magnetization vs temperature data for 30 at.% Y along the *a* axis.

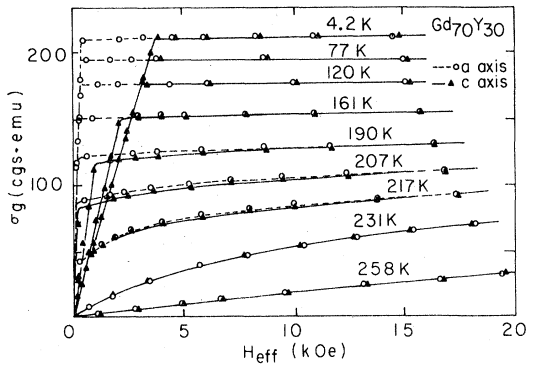

FIG. 6. Isothermal magnetization vs effective field for 30 at.% Y single crystals.

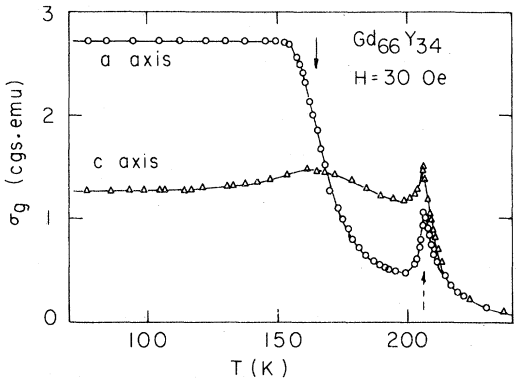

FIG. 8. Low isofield magnetization vs temperature data for 34 at.% Y single-crystal samples.

but below this temperature a new phenomenon is seen where the a-axis moment shows a second concave upward Curie-Weiss growth down to a second Curie temperature T_C^1 of 205.5 K, a result which suggests "double" ferromagnetism. A model was suggested in Ref. 8 which places the moments on the surface of a cone around the c axis at T_C (218.8 K) with the basal plane component random down to T_C^1 (205.5 K) below which simple ferromagnetism exists. The falloff of the c-axis moment below 205.5 K is thought to be a manifestation of growing anisotropy with the basal plane becoming the easy direction of magnetization. Results of measurements of the anisotropy for a spherical single-crystal sample are shown in Fig. 3. At 210.3 K, the proposed cone regime, the easy direction is along the c axis as might be expected while the data at 189.7 K show that the easy direction here is in the a-axis direction. The falloff of the c-axis moment below 205.5 K is attributed to twofold anisotropy which increases with decreasing temperature. These data are compatible with the proposed cone model.

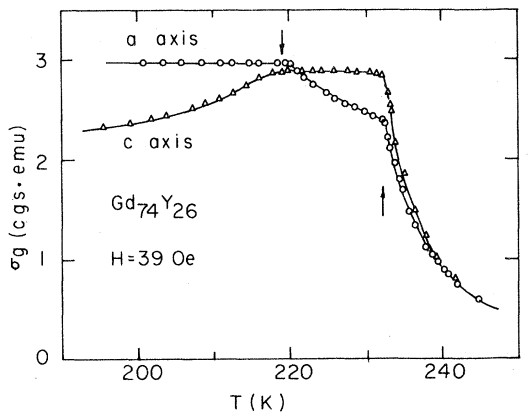

FIG. 7. Low isofield magnetization vs temperature data for 26 at.% Y single crystals.

In Fig. 4 we show c-axis isofield magnetization data for the 30 at.% Y sample. Internal fields have been used in the plot and it appears that 200 Oe is sufficient to cause the two ordering temperatures to coalesce so as to eliminate the conical phase. Similar data along the a axis are shown in Fig. 5. It appears that one kOe is needed to overcome the free pole domain effects in this crystallographic direction while 4 kOe is required to overcome both free pole and anisotropy effects in the c-axis case. Isothermal magnetization data for the 30 at.% Y sample are shown in Fig. 6. Here the dashed curves for the a-axis data show this to be the easy direction at low temperatures.

We turn next to low isofield magnetization data for 26 at.% Y as shown in Fig. 7. Here the results are just like those for 30 at.% Y described above. The highest ordering temperature, T_C, is 232.3 K and T_C^1 is 218.8 K which are both higher than those for 30 at.% Y as expected because of the higher Gd content.

In Fig. 8 the low isofield magnetization data for 34 at.% Y single crystal samples are shown. The onset of the helical phase at a T_N of 206 K can be seen in both the c-axis and a-axis directions. The c-axis moment shows a broad maximum at 163 K which is close to the 165.0 K inflection point (T_C^1) of the a-axis data. The falloff of the c-axis moment below T_C^1 is believed the result of anisotropy with the a axis becoming more entrenched as the easy direction.

IV. SPECIFIC-HEAT RESULTS

The proposed cone model for 30 at.% Y in Gd would require specific-heat peaks at both ordering temperatures 218.8 K for T_C and 205.5 K for T_C^1. Such peaks were found close to these temperatures when the specific heat was measured with the results shown in Fig. 9. It may be recalled that pure Gd shows only the peak at the 293.6 K ordering temperature[2] with little evidence of an anomaly related to the

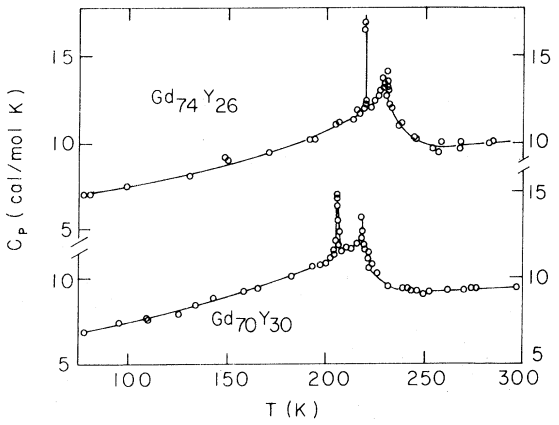

FIG. 9. Specific heat vs temperature for 26 and 30 at.% Y samples.

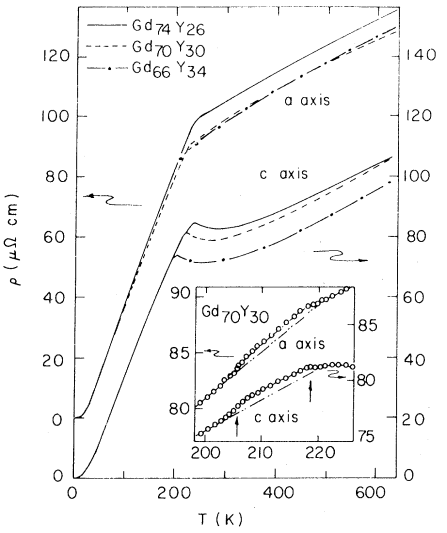

FIG. 10. Electrical resistivity vs temperature for 26, 30, and 34 at.% Y single-crystal samples. The insert at the lower right gives a greatly enlarged display of resistivity data for 30 at.% Y single-crystal samples.

anisotropy in the regime where the easy axis changes from along the c direction to the a direction near 225 K. Similar specific results were found for the 26 at.% Y sample as seen in Fig. 9. It should be noted that the specific-heat anomalies are sharp spikes corroborating the sharpness of the magnetic transitions as seen in the single-crystal isofield magnetic data.

V. ELECTRICAL RESISTIVITY RESULTS

Single-crystal samples about $1.5 \times 1.5 \times 12$ mm^3 were cut from the single-crystal buttons for electrical resistivity measurements. Results for the three single-crystal systems containing 26, 30, and 34 at.% Y are shown in Fig. 10. The residual resistivities and other resistivity parameters are given in Table I. The larger residual resistivities for a-axis samples compared to c-axis samples arise from Fermi-surface projections.[2] As can be seen in Fig. 10 the resistivities in the a-axis direction exhibit knees at the highest ordering temperature while those in the c-axis direction show broad peaks near these ordering points. In the insert of the figure we show a blowup of the resistivity in the temperature regime of interest for the 30 at.% Y sample. There is an observably higher

TABLE I. Magnetic ordering temperatures and electrical resistivity parameters for Gd-Y alloys.

at.% Y	0	2.5	5.0	7.0	8.5	10.0	15.0	20.0	22.5	25.0	26.0	27.5	30.0	34.0
T_C(K)	293.6	288.5	283.5	279.5	276.0	273.0	261.2	248.4	241.6	233.0	232.3	226.8	218.8	165.0
T_C^1(K)	225.0	234.0	241.5	247.0	248.0	248.0	244.0	235.4	229.0	221.0	219.0	214.0	205.5	
T_N(K)														206.0
$\rho_{0,a}$($\mu\Omega$ cm)											30.5	31.9	33.1	35.7
$\rho_{0,c}$($\mu\Omega$ cm)											24.3	25.9	28.1	28.8
$\rho_{\text{mag},a}$($\mu\Omega$ cm)											83.6	80.3	77.0	74.3
$\rho_{\text{mag},c}$($\mu\Omega$ cm)											54.0	52.0	50.9	43.5
$\left.\frac{d\rho}{dT}\right\|_a^{600}$ ($\mu\Omega$ cm/deg)											0.081	0.081	0.081	0.087
$\left.\frac{d\rho}{dT}\right\|_c^{600}$ ($\mu\Omega$ cm/deg)											0.084	0.086	0.088	0.087

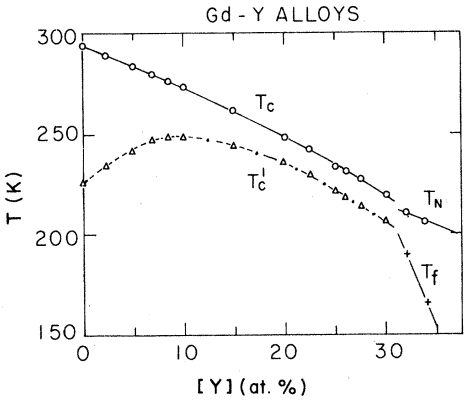

FIG. 11. Partial magnetic phase diagram for Gd-Y alloys.

resistivity for both samples in the so-called cone region above the lower ordering temperature, T_C^1. In the c-axis direction the small broad peak in the resistivity at the highest ordering temperature is just like that found for pure Gd.[2] As might be expected the electrical resistivity above the highest ordering temperature is higher for the samples of higher Gd content reflecting higher spin-disorder scattering. Since the 34 at.% Y sample displays antiferromagnetism from 165 to 206 K it shows some departure in resistivity from the other two samples in the c-axis direction as shown in the figure. The effect is not large, however.

The magnetic phase diagram for Gd-Y is shown in Fig. 11. There is a jump upward for the T_N to T_C highest ordering temperature curve near where one might have expected a Lifshitz point; this has been discussed by Legvold *et al.*[7] Below the T_C^1 and T_f lines simple ferromagnetism is found. Between T_N and T_f the samples exhibit a helical magnetic structure. Between T_C and T_C^1 we propose the conical phase in which the moments lie on a cone with the basal plane component random. Below about 10 at.% Y the samples are like Gd in their magnetic behavior.

VI. DISCUSSION

The outstanding observation is the "double" ferromagnetism found for samples with Y content from about 10 to 30 at.%. The fact that internal fields of over 200 Oe are sufficient to suppress the phenomenon and that magnetization data on single crystals are needed to observe this magnetic phenomenon explains why it was overlooked in earlier investigations. There is a hint that this phase might explain the electron spin resonance observations of Popplewell and Tebble[3] who proposed that their data indicated the presence of two phases in a temperature range near the critical regime observed here.

It will be helpful to have the results of neutron scattering experiments now underway.

ACKNOWLEDGMENTS

The authors have benefited from discussions with B. N. Harmon, S. H. Liu, and P. Burgardt. One of us (T.I.) acknowledges the support given by the Ministry of Education of Japan. The technical assistance given by R. Whetstone in the preparation of single crystals is gratefully acknowledged. Operated for the U.S. Department of Energy by Iowa State University under Contract No. W-7405-Eng-82. This research was supported by the Director for Energy Research, Office of Basic Energy Sciences, Grant. No. WPAS-KO-02-02-02.

---

*Permanent address: Department of Physics, Shimane University, Matsue-Shi, Shimane-Ken · 690, Japan.

[1]W. C. Thoburn, S. Legvold, and F. H. Spedding, Phys. Rev. 110, 1298 (1958).

[2]A recent review is given in *Ferromagnetic Materials*, edited by E. P. Wohlbarth (North-Holland, Amsterdam, 1980), Vol. 1, Chap. 3.

[3]J. Popplewell and R. S. Tebble, J. Appl. Phys. 34, 1343 (1963).

[4]T. Ito, H. Fuji, and T. Okomoto, J. Phys. Soc. Jpn. 35, 1253 (1973).

[5]D. T. Nelson and S. Legvold, Phys. Rev. 123, 80 (1961).

[6]R. M. Bozorth, J. Appl. Phys. 38, 1366 (1967).

[7]S. Legvold, P. Burgardt, and B. J. Beaudry, Phys. Rev. 22 2573 (1980).

[8]S. Legvold, T. Ito, and B. J. Beaudry, Phys. Rev. Lett. 45, 1275 (1980).

[9]H. E. Nigh, J. Appl. Phys. 34, 3323 (1963).